Ligand effects on the redox behavior of bimetallic tungsten(0)/ferrocene(II) complexes

Abby Moore, Kyle Shufelt, Benjamin G. Janesko, Kayla N. Green *

Department of Chemistry, Texas Christian University, 2800 S. University Dr., Fort Worth, TX 76129, United States

A B S T R A C T

This work presents a synthesis of bimetallic tungsten(0)/ferrocene(II) complex dppf[W(CO)$_3$PMe$_3$] and detailed comparisons of the redox behavior of dppf[W(CO)$_3$PMe$_3$], dppf[W(CO)$_4$], and dppf[W(CO)$_3$CH$_3$CN]. Reaction of PMe$_3$ with dppf[W(CO)$_3$CH$_3$CN] in dichloromethane under an inert atmosphere yields dppf[W(CO)$_3$PMe$_3$]. Slow cooling of the column purified product yields yellow blocks suitable for X-ray diffraction analysis. Structural, spectroscopic, electrochemical, and computational studies show that all three complexes have multiple redox events corresponding to tungsten and ferrocene oxidation. The complexes' distal tungsten ligands tune the first redox event over a broad range, from −37 to −200 meV versus ferrocene. Computational studies suggest that the ligand tunes the tungsten moiety's redox potential, changing the first redox event from ferrocene(II) oxidation to tungsten(0) oxidation. This bimetallic complex is thus an interesting candidate for redox-based sensing architectures.

© 2014 Elsevier Ltd. All rights reserved.

1. Introduction

Ferrocene (Fc) derivatives have received substantial attention as electrochemical biosensors. Their redox potential can significantly shift when a molecule of interest approaches the ferrocene core [1–16]. Table 1 illustrates that the Fe$^{III/II}$ potential of ferrocene derivatives is sensitive to substituents on cyclopentadienyl (Cp). Electron donating (withdrawing) Cp substituents increase (decrease) the electron density on the iron center and yield negative (positive) shifts in redox potential. Several previous studies have treated ferrocene substituent effects [4,17–19] and bimetallic diphenylphosphinoferrocene (dppf) complexes [20–24]. Relatively few studies treat the detailed redox chemistry of bimetallic dppf complexes.

We report the first structural characterization of dppf[W(CO)PMe$_3$] (complex **3**, Chart 1) and compare its electrochemical behavior to known complexes **1** and **2**. The complexes' CO bond lengths and vibrational frequencies serve as secondary probes of ligand electron donation. The tungsten ligands' electron donor ability appears to control the redox properties, with different ligands tuning the first redox event over ~140 meV.

2. Material and methods

All reagents were purchased from commercial sources and used as received unless noted. Complex **2** was produced according to the methods reported by Hsu et al. [20,21].

2.1. Physical methods

A Varian Mercury 300 spectrophotometer was utilized to obtain the NMR spectra in deuterated solvent as specified in the sections below. UV–Vis spectra were collected on an Agilent 8453 UV–Vis spectrometer using quartz cells, and infrared spectra were obtained using a Midac Corporation FT-Infrared spectrometer.

2.2. Synthesis of 1,1′-bis(diphenylphosphine)ferrocene trimethylphosphine tungsten tricarbonyl] (3)

A solution of **2** (0.517 mmol, 0.446 g) and trimethylphosphine (0.8 mmol,0.8 mL) was placed in a Schlenk flask under a nitrogen blanket. Degassed CH$_2$Cl$_2$ (15 mL) solvent was added. The resulting yellow solution was stirred for 20 h. The solvent was removed under reduced pressure yielding a mixture of crude products. Products were separated via chromatography give the desired product in 89% yield (0.414 g). Chromatography used a silica column in open air and a 1:1 ratio of CH$_2$Cl$_2$: n-hexane as solvent. Crystals suitable for X-ray diffraction were obtained by re-dissolving the

* Corresponding author. Tel.: +1 817 257 6220; fax: +1 817 257 5851.
E-mail address: kayla.green@tcu.edu (K.N. Green).

Table 1
Measured $Fe^{III/II}$ redox potential of representative Fc derivatives.

Complex	$E_{1/2}$ (mV)
1,1′-Dibromoferrocene	337
Ferrocene (Fc)	0
Decamethylferrocene [Fe(Cp*)$_2$]	−499

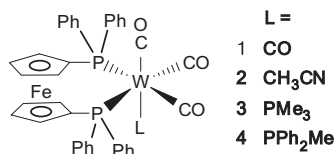**Chart 1.**

product in a minimum amount of CH_2Cl_2 and cooling in a refrigerator for four days. IR spectrum (KBr pellet) ν_{CO}/cm^{-1}:1927, 1846, 1831. ^1H NMR (300 MHz, CD_3Cl, δ/ppm): 7.62–7.32 (20H, m), 4.36 (2H, m), 4.13 (2H, m), 1.02 (9H, m). ^1H NMR (300 MHz, DMSO-d$_6$, δ/ppm): 7.47 (20H, m), 4.472 (2H, m), 4.17 (2H, m), 0.90 (9H, m). ^{31}P NMR spectrum (CD_3Cl) δ/ppm: −43.4 (t, J_{P-P} = 25 Hz, J_{W-P} = 232 Hz) ppm, 18.3 (d, J_{P-P} = 23 Hz, J_{W-P} = 214 Hz) ppm.

2.3. Structure solution and refinement

A yellow block crystal of **3** (CCDC 967367) with approximate dimensions of 0.080 mm × 0.130 mm × 0.410 mm, was used for the X-ray crystallographic analysis. The X-ray intensity data were measured on a Bruker SMART 1000 CCD system equipped with a graphite monochromator and a Mo fine-focus tube (λ = 0.71073 Å). A total of 2400 frames were collected. The total exposure time was 13.39 h. The frames were integrated with the Bruker SAINT Software package using a SAINT algorithm. The integration of the data using a monoclinic unit cell yielded a total of 174528 reflections to a maximum θ angle of 36.41° (0.60 Å resolution), of which 18354 were independent (average redundancy 9.509, completeness = 99.7%, R_{int} = 3.95%, R_{sig} = 3.27%) and 14612 (79.61%) were greater than $2\sigma(F^2)$. The final cell constants of a = 11.3247(5) Å, b = 22.5717(9) Å, c = 15.0822(6) Å, β = 101.971(2)°, volume = 3771.4(3) Å^3 are based upon the refinement of the XYZ-centroids of reflections above $20\sigma(I)$. Data were corrected for absorption effects using the multi-scan method (SADABS). The calculated minimum and maximum transmission coefficients (based on crystal size) are 0.3141 and 0.7501. The occupancy of the solvent was refined as a free variable (converged at 0.25808).

The structure was solved and refined using the Bruker SHELXTL Software Package, using the space group $P121/n1$, with Z = 4 for the formula unit, $C_{40.25}H_{37.50}Cl_{0.50}FeO_3P_3W$. The final anisotropic full-matrix least-squares refinement on F^2 with 463 variables converged at R_1 = 3.32%, for the observed data and wR_2 = 7.04% for all data. The goodness-of-fit was 1.065. The largest peak in the final difference electron density synthesis was 4.822 e Å^{-3} and the largest hole was −1.129 e Å^{-3} with an RMS deviation of 0.169 e Å^{-3}. On the basis of the final model, the calculated density was 1.619 g cm^{-3} and $F(000)$, 1826 e−.

2.4. Electrochemistry

Cyclic voltammograms were acquired at room temperature using a BASi-C3 potentiostat equipped with a 3.0 mm glassy carbon working electrode, a platinum wire auxiliary electrode, and Ag/AgNO$_3$ reference electrode filled with 0.01 M AgNO$_3$ in 0.1 M

[Bu$_4$N][BF$_4$] in CH$_3$CN. Measurements were performed under a blanket of nitrogen in 0.1 M [Bu$_4$N][BF$_4$] electrolyte in CH$_3$CN. Measurements used a scan rate of 100 mV/s. Crystalline solid **3** required treatment with a mortar and pestle prior to dissolution. Ferrocene was used as an internal standard and reported relative to NHE (Fc/Fc$^+$ = +692 mV versus NHE) [25].

2.5. Computational methods

All calculations use the GAUSSIAN 09 suite of programs [26]. Calculations use nonrelativistic generalized Kohn–Sham density functional theory [27]. The noninteracting Kohn–Sham reference state wavefunction is expanded using the LANL08 basis set and relativistic effective core potential on W and Fe, and the recommended 6-311+G(d) basis on other atoms [28]. Basis sets are taken from the EMSL Basis Set Exchange [29,30]. Calculations on open-shell systems are performed spin unrestricted [31]. Stability analysis is performed on the Kohn–Sham wavefunctions [32], and the most stable SCF solution is used unless noted otherwise. DFT calculations use the local spin-density approximation LSDA [30], B3LYP [33,34], M06 [35], or ωB97X-D [36] approximate exchange–correlation functionals. All calculations use the self-consistent reaction field model for continuum acetonitrile solvent [37,38]. Calculations use M06/LANL08 geometries, vibrational frequencies, and free energy corrections. (Some test calculations use M06/LANL2DZ geometries.) Starting geometries of all complexes are taken from crystal structures and reoptimized. Geometries are optimized from the most stable electronic state. Calculated harmonic vibrational frequencies are empirically rescaled by a factor 0.9679 before comparison to experiment, following Ref. [39]. The Gibbs free energy in solution is taken as the total energy evaluated in the continuum solvent, plus ideal gas, rigid rotor, and quasiharmonic oscillator zero-point and thermal corrections evaluated at 298 K from the geometry and vibrational frequencies evaluated in continuum solvent. Put another way, the Gibbs free energy of each species is simply taken as the "Sum of electronic thermal and Free Energies" printed by GAUSSIAN 09 from a geometry optimization + vibrational frequency calculation in continuum solvent. Refs. [40–42] discuss the validity of this approach. Phenyl groups on the dppf ligand are replaced with methyl for computational convenience. Redox potentials are computed as the difference in Gibbs free energies calculated with different electron number. For example, ferrocene's $Fe^{III/II}$ redox potential is computed as the Gibbs free energy of ferrocene with charge = 1, spin multiplicity = 2; minus the Gibbs free energy of ferrocene with charge = 0, spin multiplicity = 1. Redox potentials are evaluated versus the calculated redox potential of ferrocene [43], and are compared to the experimental $E_{1/2}$ in Table 1 and the experimental Epa in Table 5. Pictures of calculated geometries use color coding C(gray), N(blue), H(white), O(red). Bond orders are drawn as a guide to the eye. Calculated spin densities are plotted with isovalue 0.0004 au.

3. Results and discussion

3.1. Structural studies

Previous studies have shown that 1,1′-bis(diphenylphosphino)ferrocene coordinates as a bidentate ligand to form octahedral tungsten complexes [11,20,21,24,44–46]. There is limited literature focusing on the redox behavior of these bimetallic systems. The current literature attributes the observed redox behavior of these systems to Fe(II), not to W(0) [24]. Here we investigate a series of dppf[W(CO)$_3$L] complexes **1**–**3** (Chart 1) [21,24]. We report the first full structural and spectroscopic characterization of **3**; and a systematic comparison of the shifts in CO bond length,